arXiv:0706.4182v3 [hep-ex] 25 Jul 2007

Experimental tests of small-x QCD

David d'Enterria
CERN, PH-EP
CH-1211 Geneva 23, Switzerland



Current and future experimental studies of the high-energy limit of QCD, dominated by non-linear gluon dynamics in the low-x sector of the hadron wavefunctions, are presented. Results at HERA (proton) and RHIC (nucleus) pointing to the possible onset of parton saturation phenomena, and perspectives at the LHC and new proposed DIS facilities are outlined.

Keywords: QCD, low-x, gluon saturation, HERA, RHIC, LHC.

1 Introduction

Gluons provide the dominant contribution to hadronic scattering cross sections at high-energies. Deep-Inelastic (DIS) experiments of electrons off protons at the HERA collider at DESY have shown that for values of the parton momentum fraction $x = p_{parton}/p_{proton} \lesssim 0.01$, the proton wavefunction is basically purely gluonic (Fig. 1). This is so, because gluons are "cheap" to radiate: the probability of emitting a gluon increases as $\propto \alpha_s \ln(Q^2)$ and $\propto \alpha_s \ln(1/x)$ according to the standard linear QCD evolution (DGLAP [1] and BFKL [2] resp.) equations. As a matter of fact, for decreasing values of x the gluon density increases so fast that unitarity would be ultimately violated, even for processes with large virtualities $Q^2 \gg \Lambda^2_{QCD}$. The theoretical expectation [3,4] is that at some small enough value of x ($\alpha_s \ln(1/x) \gg 1$) non-linear gluon-gluon fusion effects – not accounted for in the DGLAP/BFKL equations – will become important and will tame the growth of the parton densities. The onset of saturation in the proton (or in a nucleus with A nucleons) is expected for parton momenta $Q^2 \lesssim Q^2_s$ where Q_s is a dynamical "saturation scale" [3,4] which depends on the transverse size (πR^2) of the hadron:

$$Q^2_s(x) \simeq \alpha_s \frac{1}{\pi R^2}\, xG(x,Q^2) \sim A^{1/3}\, x^{-\lambda} \sim A^{1/3}(\sqrt{s})^{\lambda} \sim A^{1/3} e^{\lambda y}, \qquad (1)$$

with $\lambda \approx 0.25$ [5]. Eq. (1) tell us that Q_s grows with the energy of the collision, $\sqrt{s}$, or equivalently, with the rapidity of the parton $y = \ln(1/x)$. The nucleon number A dependence implies that, at equivalent energies, saturation effects will be amplified by factors as large as $A^{1/3} \approx 6$ in heavy nuclear targets ($A = 208$ for Pb) compared to protons. The regime of high gluon densities is often described in terms of the colour-dipole [6,7] or "Colour Glass Condensate" (CGC) [8] effective theories, with the corresponding non-linear BK/JIMWLK [9,10] evolution equations.

2 Gluon saturation at HERA ?

Although the arguments for saturation are well justified theoretically, no strong deviation from the linear QCD equations has been conclusively observed in the perturbative kinematical range

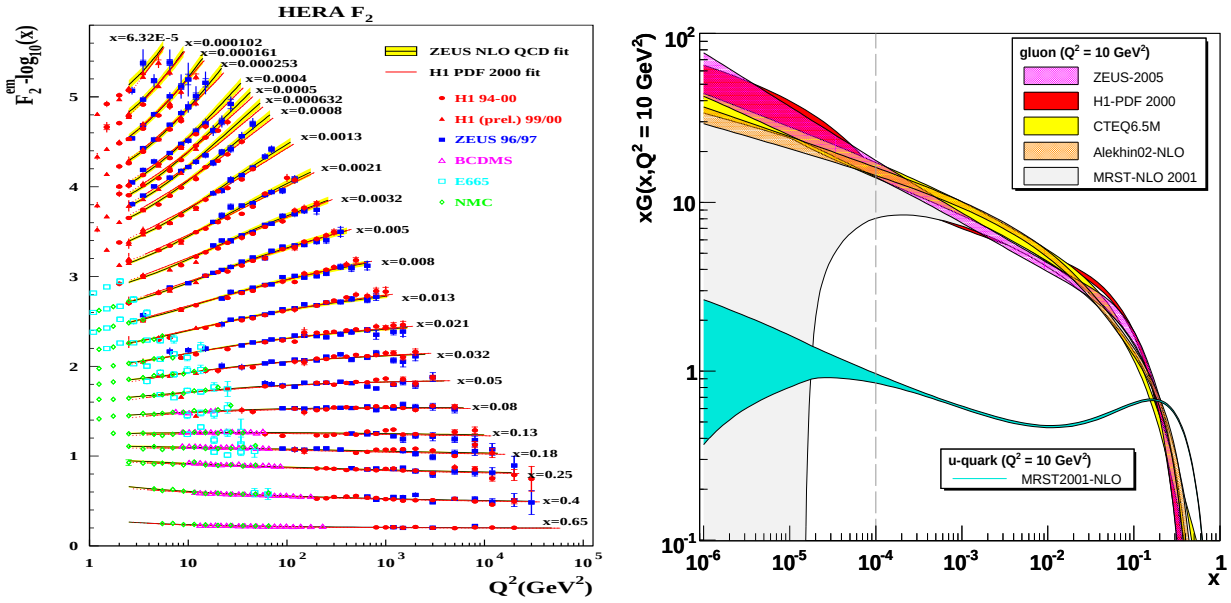


Figure 1: Left: Structure function $F_2(x, Q^2)$ measured in proton DIS at HERA ($\sqrt{s} = 320$ GeV) and fixed-target ($\sqrt{s} \approx$ 10-30 GeV) experiments. Right: Gluon distribution function in the proton, $xG(x, Q^2 = 5\ \mathrm{GeV}^2)$, derived from DGLAP-based analyses of F_2 scaling violations (for comparison, the bottom curve shows the u quark PDF).

covered at HERA. Most of the experimental observables, in particular those of more inclusive nature such as the total $\sigma_{\gamma^* p}$ cross-section $d^2\sigma/dx\,dQ^2 \approx 2\pi\alpha^2/(x\,Q^4)F_2(x, Q^2)$, are in good accord with the standard DGLAP expectations (Fig. 1). However, it is worth to note that the saturation scale at HERA energies is in a regime of relatively low virtualities, $Q_s^2 \approx 1$ GeV^2 and thus – since Bjorken x and virtuality are correlated as $x \approx Q^2/s$ – the interpretation of most of the truly low-x range probed ($x \lesssim 10^{-4}$) is "blurred" by its proximity to the non-perturbative regime. As a consequence, the gluon distribution function $xg(x, Q^2)$ indirectly obtained from the F_2 scaling violations – via $\partial F_2(x, Q^2)/\partial \ln(Q^2) \approx 10\,\alpha_s(Q^2)/(27\pi)\,xg(x, Q^2)$ – is poorly constrained below $x \approx 10^{-4}$. Different DGLAP parametrizations[a] based on DIS-only data (ZEUS-PDF, H1-PDF, Alekhin02) or on global-fits (CTEQ6.5M, MRST-NLO) yield gluon PDFs differing by factors of 3 or more (Fig. 1, right).

Notwithstanding those uncertainties, there are three empirical observations at HERA (summarized in Fig. 2) that favour a possible onset of low-x parton saturation in the proton. The leftmost plot shows the geometric scaling [7] property of inclusive σ_{DIS} which, instead of being a function of x and Q^2 separately, **for $\mathbf{x < 0.01}$** it features a single dependence on the parameter $\tau = Q^2/Q_s^2(x)$ where $Q_s(x) = Q_0(x/x_0)^\lambda$ with $\lambda \sim 0.3$, $Q_0 = 1$ GeV, and $x_0 \sim 3{\cdot}10^{-4}$. Such a scaling property is naturally explained by gluon saturation models, whereas the DGLAP approach can only reproduce it via a fine tuning of the initial parameterization of the gluon distribution used. Another piece of evidence for saturation effects at HERA is provided by diffractive processes, where the proton remains intact after the "quasi-elastic" interaction with the photon. Diffractive scattering, accounting for 10–15% of the total DIS cross-section, is characterized by colourless two-gluon exchange, and thus it constitutes a sensitive probe of the gluon densities [11]. Surprisingly, the ratio of the diffractive to total $\sigma_{\gamma^* p}$ cross-sections is found [12] to be roughly constant as a function of the center-of-mass energy W and Q^2 (Fig. 2, center). This is in disagreement with the naive pQCD expectations of an *increase* of the ratio according to $r_{\mathrm{tot}}^{\mathrm{diff}} = \sigma_{\mathrm{diff}}/\sigma_{\mathrm{tot}} \propto |xg(x, Q^2)|^2/xg(x, Q^2) \sim W^{4\lambda}/W^{2\lambda} \sim W^{2\lambda}$. The last indication of a

[a] See `http://durpdg.dur.ac.uk/hepdata/pdf3.html`

"tension" between the standard linear QCD equations and low-x HERA data comes from the longitudinal structure function, $F_L(x,Q^2)$ which at variance with F_2, is directly proportional to $xg(x,Q^2)$. The $F_L(x,Q^2)$ derived from NLO DGLAP analyses becomes unphysically negative [13] below $x \approx 10^{-4}$ for relatively small Q^2 values, whereas it is a well-behaved object in saturation models (Fig. 2, right).

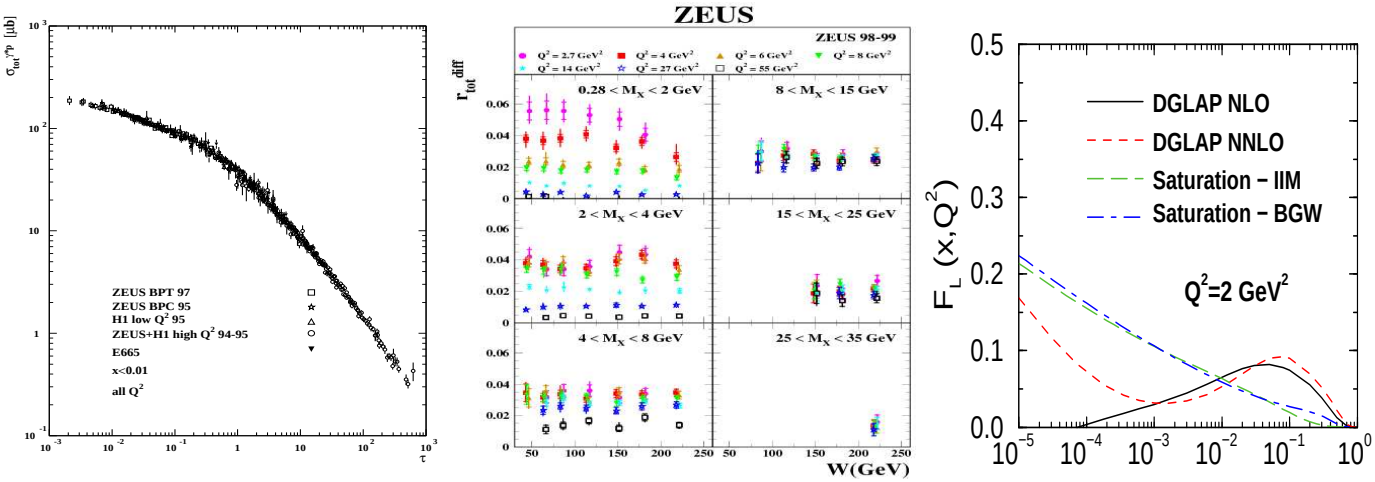


Figure 2: Hints of saturation at HERA. Left: Geometric scaling [7] of $\sigma_{\gamma^* p}$ as a function of $\tau = Q^2/Q_s^2$ for $x < 0.01$. Center: Ratio of diffractive to total DIS cross-sections [12] as a function of W and Q^2. Right: Longitudinal structure function, $F_L(x, Q^2 = 2\ \mathrm{GeV}^2)$, predicted by DGLAP [13] and saturation [7,14,15] models.

3 Gluon saturation at RHIC ?

Among the interesting observations in nucleus-nucleus (A-A) collisions at RHIC is the possible onset of parton saturation phenomena. Though nuclei at RHIC are probed at lower energies ($\sqrt{s_{NN}} = 200$ GeV) than protons at HERA, saturation effects are "amplified" thanks to the increased transverse parton density in the former compared to the latter. Two empirical observations support the Color-Glass-Condensate (CGC) predictions of a reduced parton flux in the incoming ions due to enhanced non-linear QCD effects. On the one hand, the measured hadron multiplicities [16,17,18,19], $dN_{ch}/d\eta|_{\eta=0} \approx 700$, are significantly lower than the $dN_{ch}/d\eta|_{\eta=0} \approx 1000$ values predicted by minijet [20] or Regge [21] models, but are well reproduced by CGC approaches [22]. Parton multiplicity distributions at high energies are perturbatively calculable in saturation approaches, since they are governed by a semihard saturation scale $Q_s^2 \propto \sqrt{s_{NN}}^{\lambda}$ with an exponent λ constrained by e-A data [23]. Assuming parton-hadron duality, hadron multiplicities at mid-rapidity rise proportionally to Q_s^2 times the transverse (overlap) area, a feature that accounts naturally for the experimentally observed factorization of $\sqrt{s_{NN}}$- and centrality-dependences in $dN_{ch}/d\eta|_{\eta=0}$ (Fig. 3, left).

The second manifestation of CGC-like effects in the RHIC data is the BRAHMS observation [19] of suppressed yields of semi-hard hadrons ($p_T \approx 2-4$ GeV/c) in d-Au relative to p-p collisions at increasingly forward rapidities (up to $\eta \approx 3.2$, Fig. 3, right). Hadron production at such small angles is theoretically sensitive to partons in the Au nucleus with $x_2^{min} = (p_T/\sqrt{s_{NN}})\exp(-\eta) \approx \mathcal{O}(10^{-3})$ [24]. The observed nuclear modification factor, $R_{dAu} \approx 0.8$, cannot be reproduced by pQCD calculations [24,25,26] that include the same *leading-twist* nuclear shadowing that describes the d-Au data at $y = 0$, but can be described by CGC approaches that parametrise the Au nucleus as a saturated gluon wavefunction [27,28].

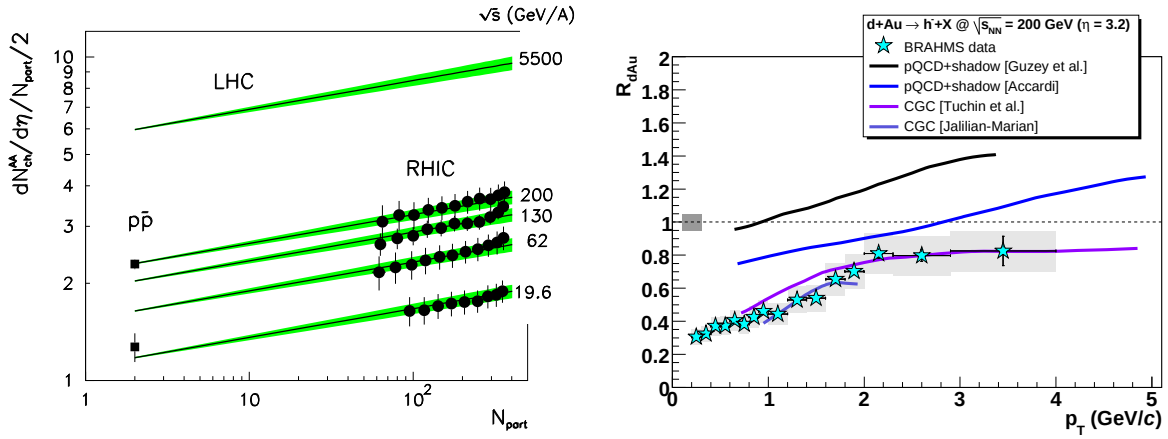


Figure 3: Hints of saturation at RHIC. Left: Normalized $dN_{ch}/d\eta|_{\eta=0}$ as a function of c.m. energy and centrality (given in terms of the number of nucleons participating in the collision, $N_{\rm part}$) measured by PHOBOS in Au-Au [16] compared with saturation predictions [23]. Right: Nuclear modification factor $R_{dAu}(p_T)$ for negative hadrons at $\eta = 3.2$ in d-Au at $\sqrt{s_{NN}} = 200$ GeV: BRAHMS data [19] compared to pQCD [24,25] and CGC [27,28] predictions.

4 Low-x QCD studies at the LHC

The Large Hadron Collider (LHC) at CERN will provide p-p, p-A and A-A collisions at $\sqrt{s_{NN}} =$ 14, 8.8 and 5.5 TeV with luminosities $\mathcal{L} \sim 10^{34}$, 10^{29} and $5{\cdot}10^{26}$ cm^{-2} s^{-1} respectively. Following Eq. (1), the relevance of low-x QCD effects will be significantly enhanced due to the increased: center-of-mass energy, nuclear radius ($A^{1/3}$), and rapidity of the produced partons [29,30]. At the LHC, the saturation momentum $Q_s^2 \approx 1$ GeV^2 (proton) – 5 GeV^2 (Pb) will be more clearly in the perturbative regime [5], hard probes will be copiously produced, and the x values experimentally accessible will be much lower than at previous colliders: $x_2 \approx 10^{-3}(10^{-6})$ at central (very forward) rapidities. All LHC experiments have interesting detection capabilities in the forward direction which will help to constrain the PDFs in the very low-x regime: (i) CMS [31,32] can measure inclusive jet and Drell-Yan production down to $x \sim 10^{-6}$ using the CASTOR calorimeter at rapidities $5.5 < \eta < 6.6$ as well as Mueller-Navelet dijets (very sensitive to non-DGLAP evolution) [33,34] separated by rapidities as large as $\Delta\eta \sim 10$, (ii) ALICE and LHCb feature a forward muon spectrometer (covering $2 \lesssim \eta \lesssim 5$) which gives them access to heavy-quark, quarkonia and gauge boson measurements [35] down to $x \sim 10^{-5}$.

The advance in the study of low-x QCD phenomena will be specially substantial in Pb-Pb collisions. In saturation models, there is a one-to-one correspondence between the effects of rapidity- and $\sqrt{s_{NN}}$-dependences, because a parton distribution boosted to higher rapidity y is equivalent to a distribution sampled in a process at higher $\sqrt{s_{NN}}$. As a consequence, the saturation physics explanation of the increasing forward suppression of semi-hard yields at RHIC will imply a significant A-A hadron suppression at LHC *mid-rapidities*. CGC predictions for charged hadron multiplicities in central Pb-Pb at 5.5 TeV [36] are $dN_{ch}/d\eta|_{\eta=0} \approx 1500$, i.e. 3-4 times lower than the pre-RHIC era results. [As a matter of fact, such low multiplicities help CMS [37] and ATLAS [38] to become very competitive experiments in the heavy-ion running mode]. Arguably, one of the cleanest way to study the low-x structure of the Pb nucleus at the LHC is via Ultraperipheral collisions (UPCs) [39] in which the strong electromagnetic fields (equivalent flux of quasi-real photons) generated by the colliding nuclei can be used for photoproduction studies at maximum energies $\sqrt{s_{\gamma N}} \approx 1$ TeV, 3-4 times larger than at HERA. Full simulation+reconstruction

studies [37,32] of quarkonia photoproduction ($\gamma\,\mathrm{Pb} \to \Upsilon\,\mathrm{Pb}$) tagged with very-forward neutrons, show that CMS can carry out detailed p_T,η measurements in the dielectron and dimuon Υ decay channels. Such processes probe x values in the nucleus as low as $x \sim 10^{-4}$ (Fig. 4, left).

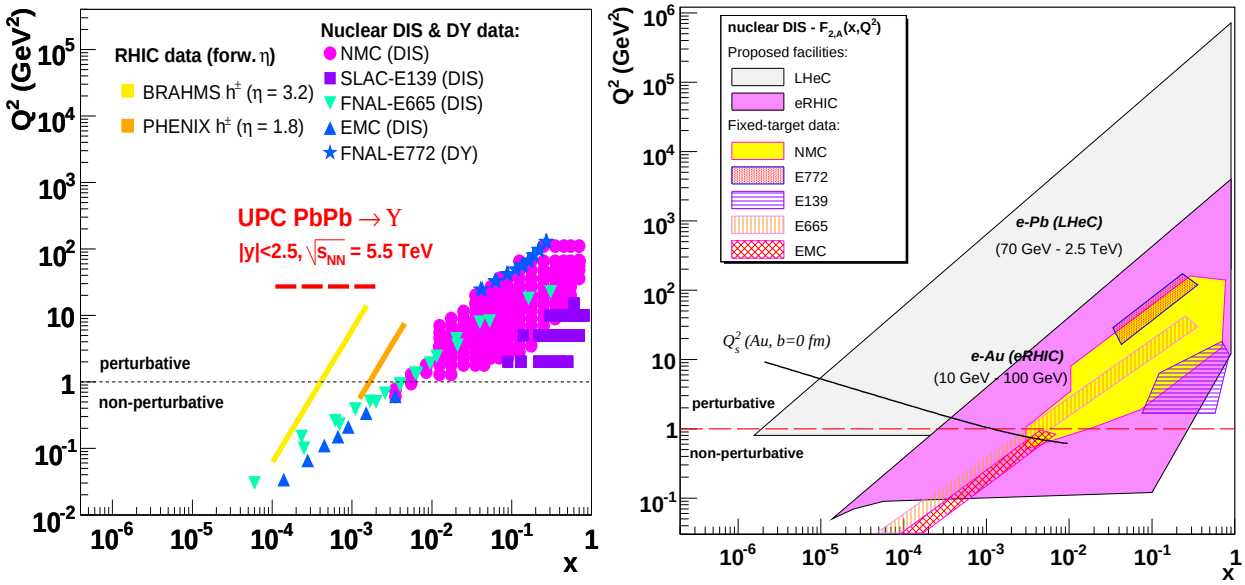


Figure 4: Kinematic (x, Q^2) plane probed in e-,γ-A processes: existing data compared to (a) UPC Υ photoproduction processes (left), and (b) new proposed nuclear DIS facilities (right): LHeC and EIC/eRHIC.

5 Proposed future deep-inelastic facilities

Two different collider projects – the Large Hadron Electron Collider (LHeC) [40] and the Electron Ion Collider (EIC) [41] – have been recently proposed to study deep-inelastic lepton-hadron (e-p, e-d and e-A) scattering for momentum transfers Q^2 as large as 10^6 GeV^2 and for Bjorken x down to the 10^{-6}. Both projects have a strong focus on the study of the low-x gluon structure of protons and nuclei and on non-linear QCD evolution. LHeC (EIC/eRHIC) proposes to add an extra E_e = 70-GeV (10-GeV) electron ring to the LHC (RHIC/JLab) proton/nucleus collider(s). In the nuclear DIS sector, LHeC (EIC/eRHIC) would allow e-A collisions at $\sqrt{s_{eN}} = 2\sqrt{E_e\,E_N} = 880$ (63) GeV. Fig. 4 right, shows the (x, Q^2) ranges accessible to both machines. Both proposed facilities would significantly extend the (meager) kinematical regime of the existing nuclear DIS data, fully mapping out the range of Bjorken-x at virtualities around the saturation scale ($Q_s^2 \approx 1$ - 10 GeV^2, indicated by the black curve in the plot) and providing very valuable insights on the high-energy limit of QCD.

Acknowledgments

It is a pleasure to thank the organizers of Moriond'07 for their kind invitation to this unique meeting. Special thanks due to François Gelis, Emmanuelle Perez, Alexander Savin, Raju Venugopalan and Graeme Watt for informative discussions and useful suggestions. This work was supported by the 6th EU Framework Programme contract MEIF-CT-2005-025073.

References

1. V.N. Gribov and L.N. Lipatov, Sov. J. Nucl. Phys. **15**, 438 (1972); G. Altarelli and G. Parisi, Nucl. Phys. **B126**, 298 (1977); Yu. L. Dokshitzer, Sov. Phys. JETP **46**, 641 (1977)
2. L.N. Lipatov, Sov. J. Nucl. Phys. **23**, 338 (1976); E.A. Kuraev *et al.*, Zh. Eksp. Teor. Fiz **72**, 3 (1977); Ya.Ya. Balitsky, L.N. Lipatov, Sov. J. Nucl. Phys. **28**, (1978) 822
3. L. Gribov, E. M. Levin and M. G. Ryskin, Phys. Rept. **100** 1 (1983)
4. A. H. Mueller and J.w. Qiu, Nucl. Phys. B **268** 427 (1986)
5. D. Kharzeev *et al.*, Phys. Lett. B **507**, 121 (2001); Nucl. Phys. A **747**, 609 (2005)
6. A. H. Mueller, Nucl. Phys. B **335** (1990) 115
7. K. Golec-Biernat, M. Wusthoff, Phys.Rev.**D 59** (1999) 014017; PR **D 60** (1999) 114023
8. See e.g. E. Iancu and R. Venugopalan, in QGP. Vol 3, Eds: R.C. Hwa *et al.*, World Scientific, Singapore, hep-ph/0303204; J. Jalilian-Marian and Y.V. Kovchegov, Prog. Part. Nucl. Phys. **56**, 104 (2006); and refs. therein
9. I. Balitsky, Nucl.Phys. **B** 463, 99 (1996); Y. Kovchegov, Phys.Rev. **D 61**, 074018 (2000).
10. J. Jalilian-Marian *et al.*, Nucl. Phys. **B504**, 415 (1997); Phys. Rev. **D59**, 014014 (1999); E. Iancu, A. Leonidov and L. McLerran, Nucl. Phys. **A692**, 583 (2001);
11. M. Arneodo and M. Diehl, arXiv:hep-ph/0511047.
12. S. Chekanov *et al.* [ZEUS Coll.], Nucl. Phys. B **713** (2005) 3
13. A. D. Martin, W. J. Stirling and R. S. Thorne, Phys. Lett. B **635** (2006) 305
14. E. Iancu, K. Itakura and S. Munier, Phys. Lett. B **590** (2004) 199
15. M. V. T. Machado, arXiv:hep-ph/0512264.
16. B.B. Back *et al.* [PHOBOS Coll.], Nucl. Phys. A **757**, 28 (2005)
17. K. Adcox *et al.* [PHENIX Coll.], Nucl. Phys. A **757**, 184 (2005)
18. J. Adams *et al.* [STAR Coll.], Nucl. Phys. A **757**, 102 (2005)
19. I. Arsene *et al.* [BRAHMS Coll.], Nucl. Phys. A **757**, 1 (2005)
20. M. Gyulassy and X.N. Wang, Comput. Phys. Commun. 83, 307 (1994)
21. A. Capella, U. Sukhatme, C.I. Tan and Van J. Tran Thanh, Phys. Rept. **236**, 225 (1994)
22. L. McLerran and R. Venugopalan, Phys. Rev. D **50** 2225 (1994), Phys. Rev. D **49** 3352 (1994), Phys. Rev. D **49** 2233 (1994).
23. N. Armesto, C. A. Salgado and U. A. Wiedemann, Phys. Rev. Lett. **94**, 022002 (2005)
24. V. Guzey, M. Strikman, and W. Vogelsang, Phys. Lett. B **603**, 173 (2004)
25. A. Accardi, Acta Phys. Hung. A22, 289 (2005)
26. D. de Florian and R. Sassot, Phys. Rev. **D69**, (2004) 074028
27. D. Kharzeev, Y. Kovchegov, K. Tuchin, Phys. Lett. B **599**, 23 (2004)
28. J. Jalilian-Marian, Nucl. Phys. A **748**, 664 (2005)
29. A. Accardi *et al.*, CERN Yellow report Hard probes in HIC at the LHC, hep-ph/0308248
30. D. d'Enterria, Eur. Phys. J. A **31** (2007) 816
31. M. Albrow *et al.* [CMS/TOTEM Coll.], CERN/LHCC 2006-039/G-124.
32. D. d'Enterria, J. Phys. **G** 34 (2007) S709.
33. A. H. Mueller and H. Navelet, Nucl. Phys. B **282**, 727 (1987)
34. S. Marzani, R. D. Ball, P. Falgari and S. Forte, arXiv:0704.2404 [hep-ph].
35. J. Baines *et al.*, hep-ph/0601164.
36. See e.g. J. L. Albacete, arXiv:0706.1251 [hep-ph].
37. CMS Coll., D. d'Enterria (ed.), "CMS Physics TDR: High Density QCD with Heavy-Ions", [CERN-LHCC-2007-009, CMS TDR 8.2-Add1], to appear in J. Phys. **G**.
38. P. Steinberg [ATLAS Coll.], arXiv:0705.0382.
39. A.J. Baltz *et al.*, J. Phys. **G** to appear, arXiv:0706.3356.
40. J. B. Dainton, M. Klein, P. Newman, E. Perez and F. Willeke, JINST **1**, P10001 (2006)
41. M.L. Miller, Moriond'07 QCD proceeds.